Geologia Croatica
Journal of the Croatian Geological Survey and the Croatian Geological Society
2026 | 79/3 | 301–319 | 15 Figs. | 4 Tabs. | www.geologia-croatica.hr

Engineering-geomorphological units of Grey Istria: lithological control on badland denudation

Vlatko Gulam[1], Marina Filipović[1,*], Iris Bostjančić[1], Davor Pollak[1], Krešimir Petrinjak[2], Stanislav Bergant[2] and Dubravko Gajski[3]

[1,*] Croatian Geological Survey, Department of Hydrogeology and Engineering geology, Sachsova 2, 10000 Zagreb, Croatia; (*corresponding author: mfilipovic@hgi-cgs.hr)
[2] Croatian Geological Survey, Department of Geology, Sachsova 2, 10000 Zagreb, Croatia
[3] University of Zagreb, Faculty of Geodesy, University of Zagreb, Kačićeva 26, 10000 Zagreb, Croatia

doi: 10.4154/gc.2026.15

CC BY
Crossref Similarity Check

Original scientific paper

Article history:
Manuscript received: March 18, 2026
Revised manuscript accepted: July 22, 2026
Available online: October 27, 2026

Abstract

Grey Istria is characterized by extensive badland development within a marl-dominated Palaeogene foreland-basin succession. This succession comprises hemipelagic Globigerina marls and the overlying Istrian flysch, whose lithological composition and rock-mass structure, together with slope geometry and surface-water concentration, influence slope degradation and denudation. The presented study aims to evaluate the preliminary engineering-geomorphological (EG) subdivision of the marl-dominated Palaeogene foreland-basin succession by integrating sample-scale and outcrop-scale evidence. The proposed EG units were evaluated using marl durability testing, calcimetry, Geological Strength Index (GSI) assessment, and denudation measurements from representative badland test plots. Four EG units were defined and tested in order to examine whether this subdivision is supported by measurable differences in material properties and field behaviour. The results confirm that the proposed classificaton of EG units is justified both at the sample scale, through durability and calcimetric analyses, and at the outcrop scale, through GSI-based characterization and denudation measurements on badlands. The novelty of this study lies in the first engineering-geomorphological classification of the marl-dominated Palaeogene foreland-basin succession of Grey Istria, developed according to the geomorphological behaviour of its lithological units. The proposed classification provides a framework for future research on badland development, denudation, and engineering-geomorphological mapping.

Keywords: Engineering-geomorphological units, marl durability, denudation, flysch, badland, Grey Istria

1. INTRODUCTION

The evolution of most landforms on Earth occurs over long geological timescales, making it difficult to observe and quantify the processes that shape them directly (HOWARD & KERBY, 1983). In contrast, Badlands, with their steep slopes, sparse or absent vegetation, high drainage density, and intense surface erosion, provide a unique opportunity to study geomorphological processes in near real time, at spatial and temporal scales relevant to both field experimentation and engineering applications (WAINWRIGHT & BRAZIER, 2011). Formed in soft sedimentary and clay-rich materials that undergo rapid surface changes, badlands serve as natural laboratories for investigating interactions among lithology, climate, vegetation, and human activity.

Badlands are globally widespread and occur under a variety of climatic and geological settings – from the Mediterranean region to arid and semi-arid zones of Africa, Asia, and the Americas (BRYAN & YAIR, 1982; GALLART et al., 2002; HARVEY, 2004). Geomorphologically, they are broadly defined as landscapes shaped by the combined effects of piping, erosion, and mass movement, acting together with fluvial processes (BRYAN & YAIR, 1982), typically affecting fine-grained sedimentary rocks such as marls and shales. These landscapes are often characterized by high sediment yields, rapid incision, and frequent slope failures, making them highly dynamic systems.

Among the various factors controlling badland development, lithology plays a particularly important role (KASANIN-GRUBIN & BRYAN, 2007; MORENO-DE LAS HERAS & GALLART, 2018). Numerous studies have demonstrated that the mechanical and hydrological properties of the substrate, such as strength, permeability, and susceptibility to weathering, strongly influence the initiation, evolution, and persistence of badland morphology (BRYAN & HARVEY, 1985; BOUMA & IMESON, 2000). Marl, in particular, is characterized by low to moderate uniaxial compressive strength, low permeability, and high susceptibility to mechanical weathering processes, such as repeated wetting–drying, heating–cooling, and freeze–thaw cycles. These cycles cause repetitive swelling and shrinkage, leading to fissuring, surface crusting, and eventual disintegration. The resulting material is highly erodible, especially where protective vegetation cover is either sparse or absent.

Although this study focuses primarily on lithological and material controls, badland development and denudation result from the interaction of multiple factors, including slope geometry, bedding orientation, hydrological conditions, drainage concentration, vegetation cover, and channel–toe contact. These factors are therefore considered where necessary to interpret the observed field behaviour, although their systematic evaluation lies beyond the main scope of this study.

In Croatia, badlands are predominantly associated with flysch and flysch-like materials of Grey Istria (BOSTJANČIĆ et al., 2022). The name "Grey Istria" refers to the characteristic grey colour of widely exposed marl outcrops, reflecting the dominance of this lithology within the Istrian flysch complex (GULAM et al., 2023). The region, located in the central part of the Istrian Peninsula, is geomorphologically characterized by steep hills and deeply incised valleys, which are frequently affected by surface erosion and mass wasting.

Within Grey Istria, several lithostratigraphic units have already been delineated based on sedimentological and stratigraphic characteristics (BERGANT et al., 2003). However, these units have not yet been systematically evaluated from an engineering-geomorphological (EG) perspective, particularly with respect to their resistance to mechanical weathering, a key factor controlling surface processes and the spatial distribution of badlands.

This study addresses this gap through three primary objectives. The first objective is to define engineering-geomorphological units within the marl-dominated Palaeogene foreland-basin succession of Grey Istria. The second is to assess whether marl durability differs among the defined units using laboratory simulations of environmental weathering. The third is to examine whether the observed differences in material properties are reflected in preliminary denudation measurements from four representative badland test plots.

Calcimetry and Geological Strength Index (GSI) assessment are used as supporting analyses to characterize compositional differences and rock-mass conditions within the proposed EG units.Through the analyses presented here, two working hypotheses are tested to justify and validate the proposed EG units: (1) Denudation rates differ systematically between the predefined EG units; and (2) Marl durability differs systematically among the predefined marl-dominated EG units and provides a basis for distinguishing them.

2. STUDY AREA

Istria is the largest Croatian peninsula, situated in the westernmost part of Croatia within the northern Adriatic region. About 90 % of its territory lies within Croatia, while the remaining small portion extends over Slovenia and Italy. The Učka and Ćićarija mountains form the natural eastern boundary of the peninsula, separating Istria from the Kvarner region. The study area, referred to as Grey Istria and forming part of the Pazin Basin, covers approximately 570 km² and comprises a marl-dominated Palaeogene foreland-basin succession (Fig. 1). The region is particularly suitable for badland research because it contains the largest concentration of badlands in Croatia, exhibits locally high sediment production with practical consequences for watercourses, reservoirs, and drainage infrastructure, and is supported by an existing badland inventory and spatial datasets (GULAM et al., 2014; BOSTJANČIĆ et al., 2022) (Fig. 1).

Geologically, the Istrian Peninsula predominantly belongs to the Adriatic Foreland, while its northeastern mountainous area represents part of the External Dinarides fold-and-thrust belt, formed during the Alpine orogeny (SCHMID et al., 2008; KORBAR, 2009). Stratigraphically, Istria features Jurassic and Cretaceous limestones deposited on the Adriatic carbonate platform, separated from Paleogene foreland basin deposits by a regional unconformity and palaeokarst features (MATIČEC et al., 1996; VELIĆ et al., 2003; VLAHOVIĆ et al., 2005; OTONIČAR, 2007).

During the Paleogene, a foreland basin developed in northwestern Istria (KORBAR, 2009; PETRINJAK et al, 2026). Its sedimentary succession includes Foraminiferal limestones and the Istrian flysch (BERGANT et al., 2003; OTONIČAR, 2007).

A relatively thin interval of the so-called Transitional Beds marks a shift toward deeper foredeep environments (ŠIKIĆ & PLENIČAR, 1975; MARJANAC & ĆOSOVIĆ, 2000; TARLAO et al., 2005).

2.1. Lithologies hosting badlands

Badland development and intense erosion in Grey Istria are primarily associated with two lithological units—massive Globigerina marls and the overlying marl–sandstone alternations characteristic of the Istrian flysch. Their low infiltration capacity favours rapid surface runoff and the concentration of erosive flows, while their low durability promotes the rapid production of loose material that is subsequently removed by these flows. Previously mentioned Transitional Beds are overlain by massive Globigerina marls interpreted differently by various authors: transitional deposits (MARJANAC & ĆOSOVIĆ, 2000; ĆOSOVIĆ et al., 2008), true deep-sea sediments (JURAČIĆ, 1979), or part of the flysch formation (MARINČIĆ et al., 1996; BERGANT et al., 2020). Depending on their position within the sedimentary basin, these marls can reach thicknesses of up to 80 m (ŠIKIĆ & PLENIČAR, 1975).

Within the stratigraphic succession, the massive Globigerina marls are overlain by deposits traditionally referred to as flysch. This unit consists of alternating hemipelagic marls and various coarse-grained gravity-flow deposits, displaying a clear upward-coarsening trend. The gravity-flow deposits are predominantly turbidites, which can be subdivided into mixed carbonate-siliciclastic and purely carbonate types.

The mixed turbidites occur predominantly in the upper part of the Istrian flysch succession (BABIĆ & ZUPANIČ, 1996). They were transported from the rising Dinarides and Alps toward the east–southeast and are interpreted as deposits of low-density turbidity currents (MAGDALENIĆ, 1972; MARINČIĆ et al., 1996; BABIĆ & ZUPANIČ, 1996; BERGANT et al., 2003; HORVAT et al., 2023; PETRINJAK et al, 2026). In contrast, carbonate-rich beds, breccias, conglomerates, bioclastic arenites, and marls, indicate a north–

northeast transport direction, suggesting derivation from an uplifted carbonate forebulge located to the south (BABIĆ & ZUPANIČ, 1996).

Based on the stratigraphy, composition, and sedimentary facies, the Istrian flysch can be subdivided into three distinct units described slightly different by several authors (MULDINI-MAMUŽIĆ, 1964; MARINČIĆ et al., 1996; BABIĆ et al., 2007; PETRINJAK et al., 2021, 2026). In summary, these units can be characterized as follows: (i) Lower unit – massive Globigerina marls, (ii) Middle unit – alternating hemipelagic marl and occasional carbonate turbidites, and (iii) Upper unit – alternating mixed siliciclastic and carbonate turbidites and marls (Fig. 2).

From a structural perspective, the Globigerina marls and Istrian flysch deposits are, over large parts of the Paleogene basin, particularly in its southern and southwestern sectors, only weakly deformed and typically characterized by subhorizontal bedding. In contrast, the northeastern sector, adjacent to the Ćićarija and Učka units, represents a basin-margin structural belt that marks the transition from the gently bedded basin interior to a structurally more complex domain. Within this marginal belt, bedding commonly becomes inclined and deformed, reflecting increased deformation near the NE basin margin (Fig. 1). The influence of tectonic deformation, most notably bedding dip, on badland development has been discussed in the regional literature (GULAM et al., 2014).

Finally, it is important to emphasize that the literature cited here consistently points to the predominance of marls in Grey Istria; given that marl, owing to its high clay content, is generally of low permeability, such a lithological setting provides the fundamental hydrological precondition for concentrated overland flow and intense exogenic badland dynamics.

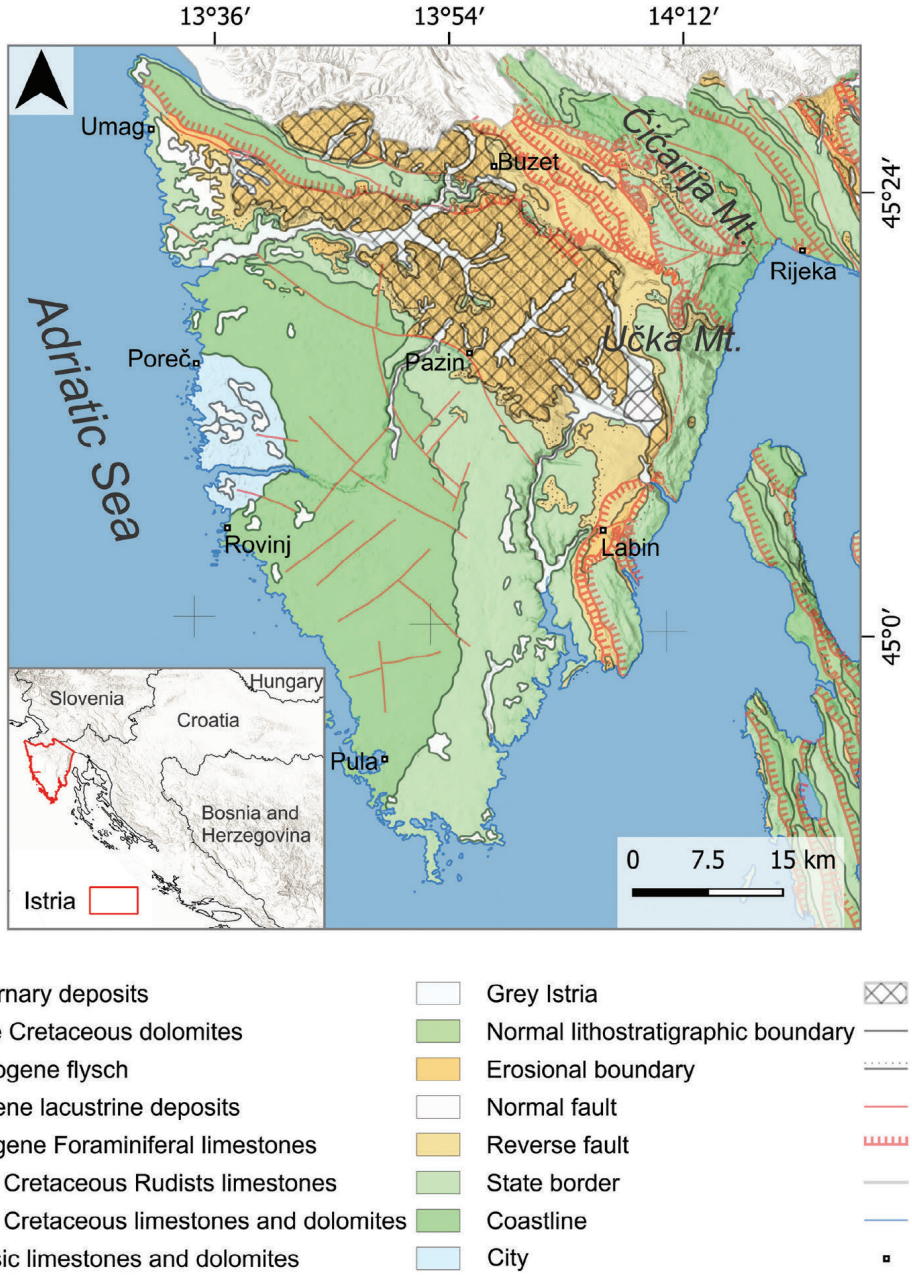


Figure 1. A geological map of the Croatian part of the Istrian peninsula at a scale of 1:300 000 (CROATIAN GEOLOGICAL SURVEY, 2009).

Geologia Croatica

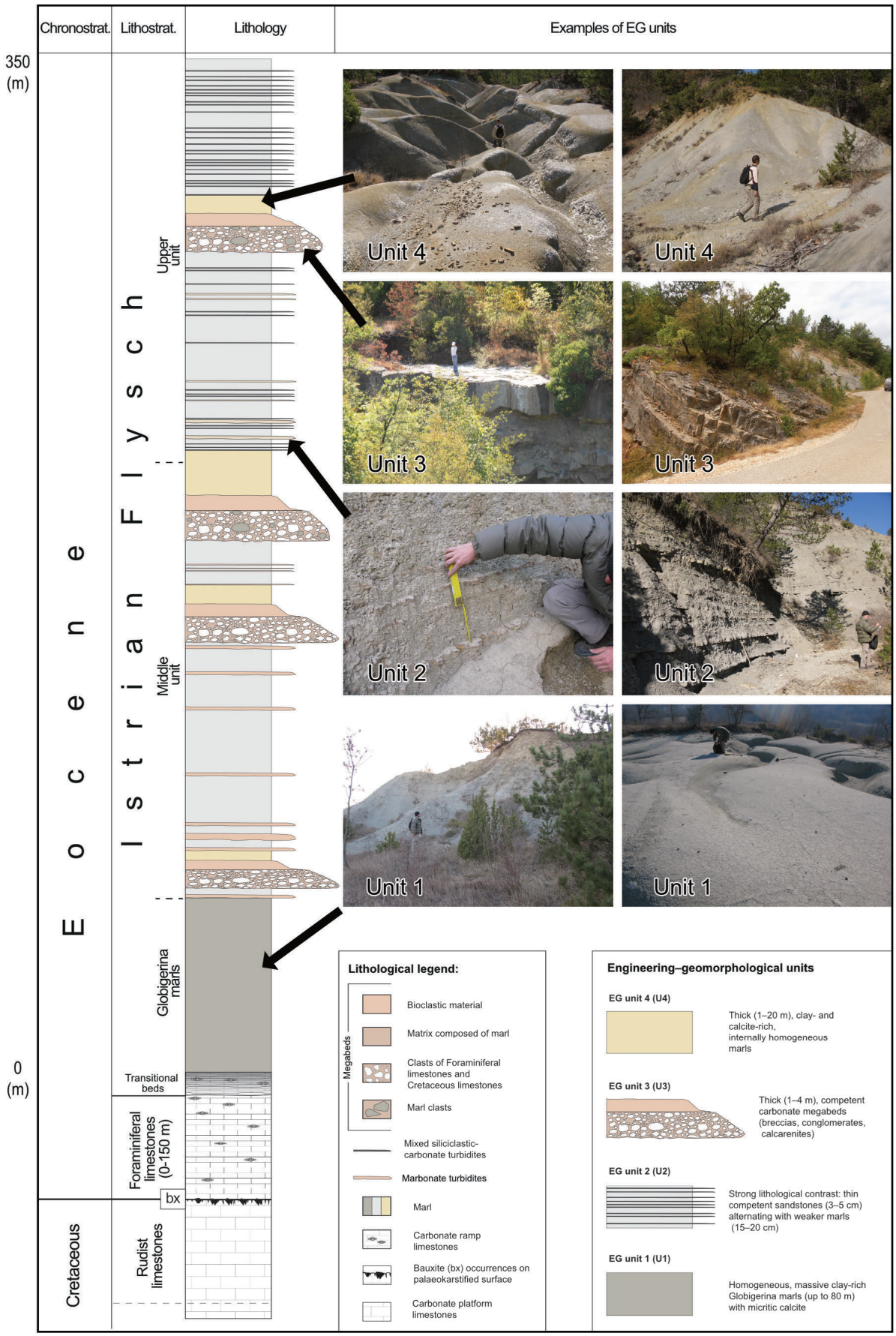


Figure 2. A schematic geological column depicting the Middle Eocene Globigerina marls and the overlying Istrian flysch succession, together with the underlying Cretaceous and Palaeogene carbonate deposits. The Transitional Beds, Foraminiferal limestones, and Cretaceous formations are not shown to scale relative to the marl and flysch succession. The positions of the preliminary engineering-geomorphological units are included for comparison with the lithostratigraphic framework; their delineation and definition are presented in Section 3.1. (modified after PETRINJAK et al. (2021)).

3. METHODS

3.1. Workflow for preliminary delineation of engineering-geomorphological units

The preliminary delineation of EG units was expert-driven and descriptive, grounded in the visual geomorphological interpretation of Grey Istria. Rather than applying a formal quantitative classification, we used a process-oriented reading of lithology-relief relationships, developed iteratively through direct field observations and complemented by desk-based analysis of remote-sensing and cartographic datasets, particularly 1:5,000-scale digital orthophotos.

Accordingly, the workflow integrated three main lines of evidence:

- extensive EG reconnaissance across Grey Istria, carried out during >10 multidisciplinary field campaigns (engineering geology, geomorphology, hydrogeology, geodesy, hydraulic engineering) between 2007 and 2012,
- systematic orthophoto interpretation (1:5,000), following the protocol previously used to inventory 5,568 badland polygons in Grey Istria (GULAM, 2012; BOSTJANČIĆ et al., 2022), combined with interpretation of existing geological maps to trace badland areas, gully networks, and—where mappable—lithostratigraphic boundaries,
- synthesis of the regional literature to constrain the exogenetic process chain and lithological controls on surface dynamics.

Following this approach, four preliminary EG units within the Istrian flysch succession were delineated: U1 (Massive Globigerina marls), U2 (Marl–sandstone alternation), U3 (Megabeds), and U4 (Thick marl intervals above the Megabeds).

The preliminary EG units were defined using a hierarchical set of qualitative field and remote-sensing criteria rather than fixed numerical thresholds. The primary criteria included the predominant lithological composition, the relative proportion and thickness of competent and incompetent members, bedding characteristics, stratigraphic and spatial occurrences, and characteristic geomorphological expression. These criteria were used to identify and differentiate the units during field observations and interpretation of orthophotos and geological maps. The main characteristics of the four preliminary EG units are summarized in Table 1.

The criteria were considered jointly, with the predominant lithology and the arrangement of competent and incompetent members serving as the primary basis for unit identification, while stratigraphic position, spatial occurrence, and geomorphological expression were used as supporting characteristics. Because individual criteria may overlap locally between units, no single characteristic was considered sufficient for unit assignment. The proposed classification is therefore expert-guided but based on an explicit and reproducible combination of geological and geomorphological observations.

The preliminary EG unit framework served as the basis for field sampling and for selecting representative badland test plots for denudation monitoring. Its coherence is subsequently evaluated quantitatively at two levels: (i) sample scale (marl durability and calcimetry) and (ii) outcrop/landform scale (denudation measurements on test plots and GSI detrmination).

3.2. Field sampling

Samples were taken predominantly from exposed bedrock on active badland faces (gully sidewalls and scarps), targeting the subsurface zone of the rock mass rather than loose surficial regolith, talus, or soil. Where natural badland exposures were absent or unsafe, equivalent lithological members were sampled on roadcuts. In all cases, visibly altered surface crusts were removed prior to sampling to expose representative rock fragments for selection.

To minimize the influence of the highly disintegrated eluvial layer, samples were collected from shallow pits (15–25 cm below the surface) using standard hand tools (spade/mattock,

Table 1. Criteria used for the identification and differentiation of the preliminary engineering-geomorphological units in Grey Istria.

EG unit	Primary lithological and thickness criterion	Bedding/layering criterion	Stratigraphic and spatial position	Characteristic geomorphological expression
U1	Massive Globigerina marls forming marl-dominated packages up to several tens of metres thick, with only rare or very thin competent interbeds	Massive to weakly bedded	Lower part of the Palaeogene foreland-basin succession, below the Istrian flysch. Spatially, U1 occurs mainly along the margins of the Pazin Basin and locally in deeply incised gullies where erosion has exposed the Globigerina marls above the Foraminiferal limestone substrate	Rounded, generally lower-angle badland slopes; predominance of sheetwash and shallow surface degradation
U2	Rhythmic alternation of thin competent sandstone beds, typically about 3–5 cm thick, and thicker incompetent marl intervals, commonly about 15–20 cm thick	Regularly bedded heterogeneous succession with a pronounced alternation of competent and incompetent members	Middle and upper parts of the Istrian flysch succession. Spatially, U2 is widespread in the central part of the basin and forms the most extensive EG unit within Grey Istria	Steep gully sidewalls, bed-controlled asymmetry, local sandstone armouring, raveling, and small slope failures
U3	Competent carbonate megabeds, generally about 1–4 m thick and locally thicker, composed of breccias, conglomerates, and bioclastic arenites	Thick, laterally persistent competent beds sharply contrasting with adjacent marl-dominated intervals	Occurring at several stratigraphic levels within the Istrian flysch succession, mainly in the central parts of the basin where the flysch succession is more fully preserved	Distinct erosional steps, local base levels, knickpoints, and strong control on gully organisation
U4	Thick marl-dominated intervals, generally 3–5 m thick and locally exceeding 15 m	Massive to weakly bedded, comparatively homogeneous marl packages	Upper part of the Istrian flysch succession, typically above carbonate megabeds. Spatially, U4 occurs mainly in the central part of the basin, where thicker upper-flysch marl intervals are preserved	Broad marl slopes and badlands with morphology similar to U1; predominance of sheetwash and relatively uniform surface lowering

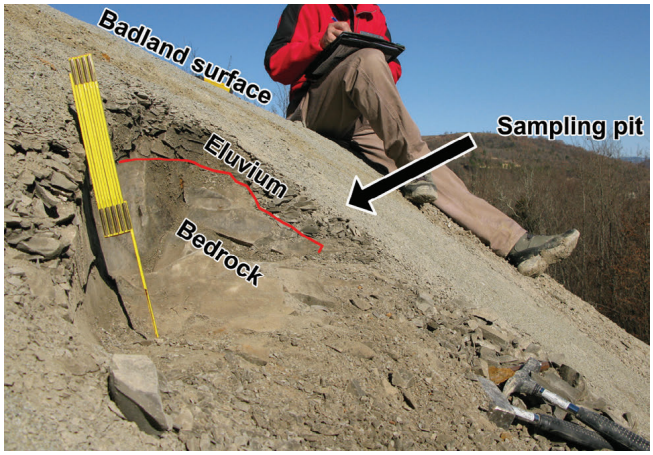


Figure 3. A sampling pit in U4 with eluvium crust and bedrock exposed.

geological hammer, chisel, and a steel pry bar). Sampling was performed after removing the surficial crumbly layer (Fig. 3).

The sampling design, stratified by EG units, aimed to capture the lithological variability relevant to durability testing. A total of 65 samples were collected from sites distributed across the study area (Fig. 4). Given the predominance of marl within the Palaeogene foreland-basin succession of Grey Istria, sampling focused primarily on the massive Globigerina marls of U1 and the less competent marl members of U2 and U4, comprising 63 samples in total. Two additional samples of competent sandstone and carbonate material from U3 were collected but excluded from subsequent laboratory analyses because their markedly higher competence made them unsuitable for direct comparison with the marl samples.

Unlike U1, U2, and U4, U3 is therefore not quantitatively evaluated in this study. Its identification as a distinct EG unit is supported primarily by field observations, lithological characteristics, and its characteristic geomorphological expression. Consequently, the quantitative analyses presented below are limited to the three marl-dominated units, whereas U3 is discussed qualitatively in relation to its role in the organisation of badland relief. All subsequent quantitative analyses were therefore conducted on U1, U2, and U4. The contrasting competence, thickness, and geomorphological role of U3 are addressed qualitatively in the Results and Discussion sections.

3.3. GSI characterization

During field mapping, we assigned a Geological Strength Index (GSI) value to each EG unit using the recommended GSI scheme for weak and complex rock masses (MARINOS, 2010). Although GSI was originally developed for tunneling and underground construction (MARINOS, 2014), in this study it is applied as a standardized, field-robust descriptor of rock-mass fabric (blockiness and discontinuity condition) that controls near-surface slope behaviour in the marl–flysch terrain of Grey Istria.

GSI assessments were performed by the same field team using the MARINOS (2010) classification scheme, and the assigned values were agreed upon jointly in order to maintain consistency among observation points. The evaluation considered rock-mass structure, degree of blockiness, lithological heterogeneity, and discontinuity surface conditions. Where field conditions fell between two chart categories, transitional GSI ranges were assigned rather than a single fixed value.

In this study, GSI is not used as a design parameter but as a comparative field index supporting the differentiation of EG units. Because GSI assessment involves expert judgement, the assigned values should be interpreted as semi-quantitative

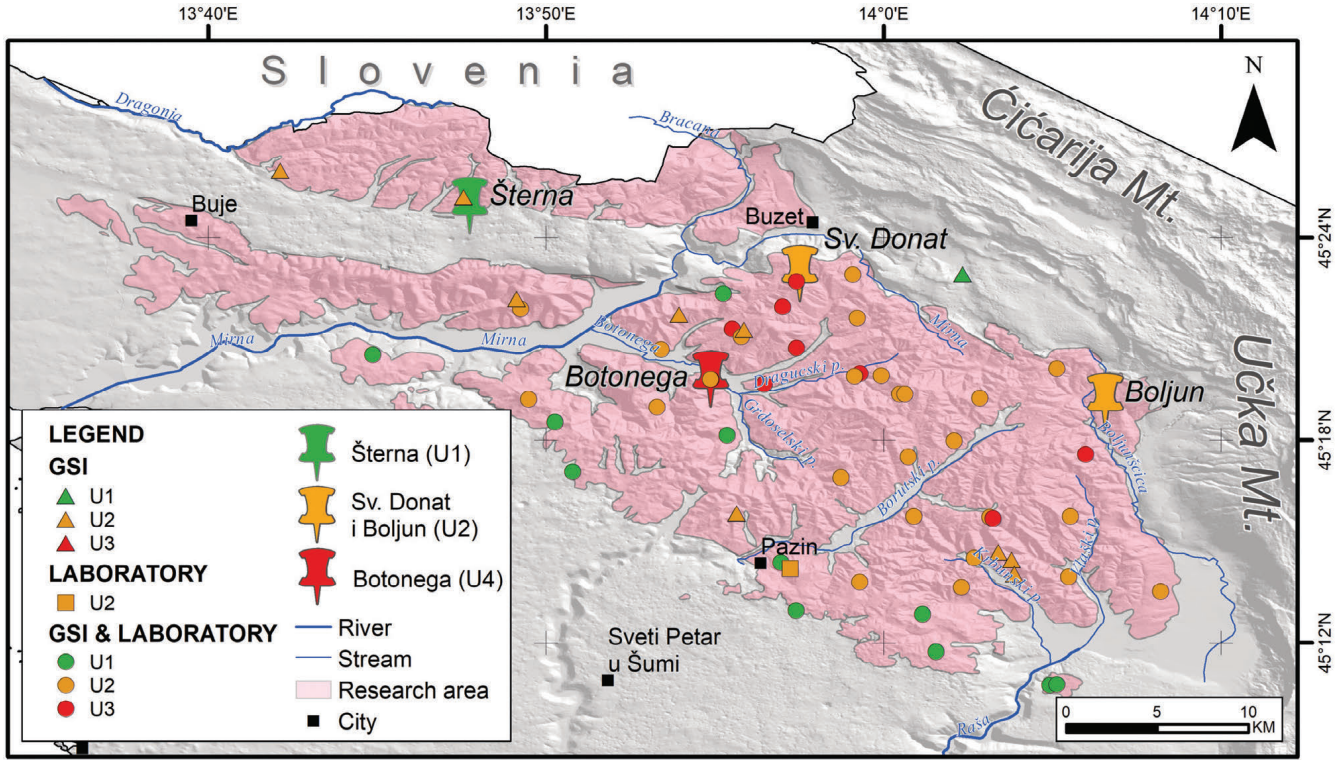


Figure 4. Field sampling locations, GSI assessment points and badland test plots.

ranges rather than exact measurements, and some evaluator-related uncertainty is therefore unavoidable.

GSI classification was performed at 55 field observation points, shown in Figure 4, largely coinciding with the sampling locations.

Accordingly, GSI is treated here as a semi-quantitative field index for comparing and stratifying EG units by their expected blockiness and degradation state, rather than as a design parameter.

3.4. Badland test plots

Denudation was monitored at four representative badland test plots – Šterna (U1), Sv. Donat (U2), Boljun (U2), and Botonega (U4) – selected to cover the range of EG units susceptible to weathering (Fig. 4). Several field methods were applied to determine denudation rates. All test plots were monitored by at least two of the following: digital photogrammetry (cm-scale DEM differencing), analogue photogrammetry (stereo pairs; DEM differencing), and profilometry (repeated micro-profile measurements). Where multiple methods overlapped, results were reported jointly to highlight method agreement and scale effects.

The Šterna badland is located in the northernmost part of Grey Istria, near the village of Šterna. The total badland area is app. 44,200 m², situated on gently dipping strata (311°/13°) and dissected into sub-areas that share a common erosional base (a stream) connected via a deeply incised gully network (Fig. 5). Large-scale digital photogrammetric measurements were carried out on a 6 m² parcel, with a slope inclination of 18° to 40°, tracking 24 points from October 2008 to January 2009 (estimated internal error ≈ 1.38 mm). Additional smaller scale digital and analogue photogrammetric measurements of a broader area were also conducted. However, monitoring was limited due to uniform surface colour (Globigerina marls) and vandalism of profilometers during the first year.

The Sv. Donat badland is located app. 2.7 km south of the City of Buzet and is named after the nearby settlement of Sv. Donat. The total badland area is app. 51,000 m² (Fig. 6). It extends along a 112–292° direction and is exposed towards the north–northeast. Its approximate length is 1,100 m, with a maximum elevation difference in the central part of around 60 m. Large-scale digital photogrammetric measurements were carried out on a 14 m² parcel, with a slope inclination of 64–68°, from October 2008 to January 2011 (estimated internal error ≈ 1.25 mm). Smaller scale analog photogrammetric



Figure 5. The Šterna badland with test plot site.

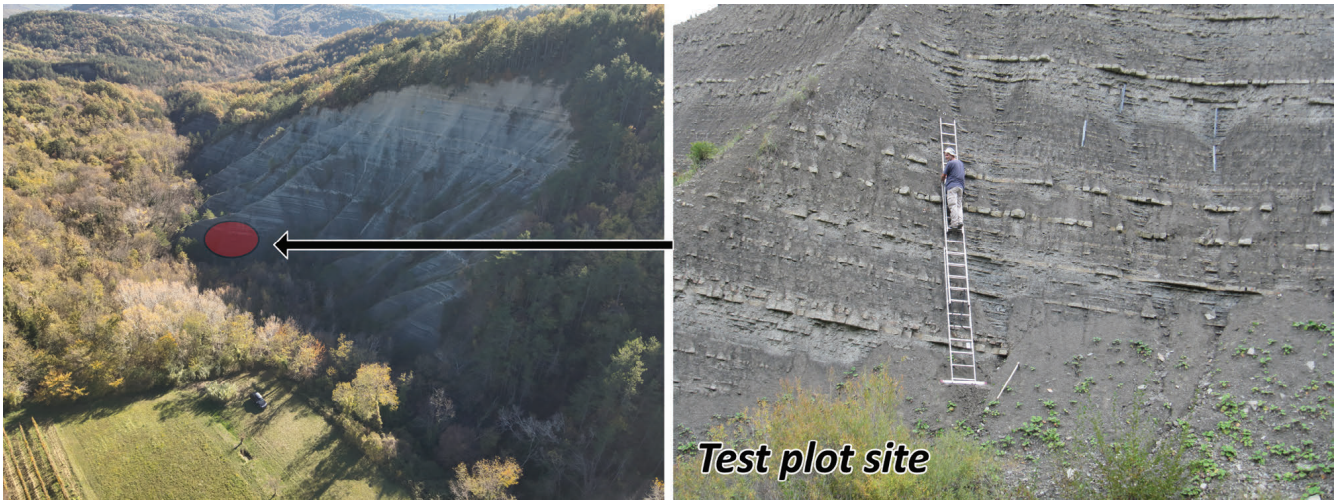


Figure 6. The Sv. Donat badland with test plot site.

measurements were conducted on a parcel of app. 175 m², with a slope inclination of 50° to 80°, measuring a total of 775 points, from October 2008 to October 2009 (estimated internal error ≈ 6.1 mm). Profilometric measurements were conducted from May 2008 to January 2011.

The Boljun badland is situated near the Boljunčica River, app. 2 km north–northwest of the small town of Boljun. The total badland area is 51,000 m² (Fig. 7). The main gully is app. 2,300 m long and extends in a 0–180° direction, while the bedding planes are oriented 244°/28°. Large-scale digital photogrammetric measurements were carried out on a 16 m² parcel, with a slope inclination of 55° to 60°, from October 2008 to December 2010 (estimated internal error ≈ 1.6 mm). Smaller scale analog photogrammetric measurements were conducted on a parcel of app. 95 m², with a slope inclination of 40° to 70°, measuring a total of 449 points, from October 2008 to December 2010 (estimated internal error ≈ 2.9 mm). Profilometric measurements were conducted from May 2008 to December 2010.

The Botonega badland is located approximately 350 m west of the Botonega dam. With a total area of app. 1,800 m², it is the smallest badland among the four testing sites (Fig. 8). Large-scale digital photogrammetric measurements were carried out on two segments, on parcels of 8.6 m² and 3.5 m², with slope inclinations of 39° and 35°, representing both sides of the badland gully. A total of 58 points were monitored on both parcels from October 2008 to January 2011 (estimated internal error ≈ 1.18 mm). Due to the gentle slope and the lack of pronounced surface features, smaller scale analogue and digital photogrammetric measurements could not be performed with sufficient accuracy. Profilometric measurements were conducted from May 2008 to January 2011.

The test plots differ in slope inclination, exposure, local morphology, monitoring duration, and the combination of measurement methods applied. Consequently, their denudation rates are not interpreted as a strictly controlled comparison in which EG unit membership represents the only variable. Instead, the plots provide representative field observations used to examine whether material-related differences among the EG units are broadly reflected in denudation patterns under different local morphometric settings.

3.5. Calcimetry

The carbonate content in marl samples, reported as wt.%, $CaCO_3$, was determined following the simplified Collins calcimeter method (HEAD, 1982). This method measures the



Figure 7. The Boljun badland with test plot site



Figure 8. The Botonega badland with test plot site.

volume of CO_2 released after adding hydrochloric acid to carbonate-bearing material, allowing the $CaCO_3$ content to be calculated from the reaction stoichiometry: $CaCO_3 + 2HCl \rightarrow CaCl_2 + H_2O + CO_2\uparrow$.

Carbonate content is used here as a first-order inverse proxy for the abundance of non-carbonate components, particularly clay minerals. This approximation assumes that calcite and clay minerals are the dominant phases in the studied marls. However, other non-carbonate minerals, such as quartz and minor feldspars, may also contribute to the bulk composition. Therefore, $CaCO_3$ values are interpreted as a simplified compositional indicator rather than as a direct quantitative measure of clay-mineral content. Calcimetry was performed on 58 samples, organized according to the EG unit framework as follows: U1 – 15 samples, U2 – 33 samples, U4 – 10 samples. These 58 samples also include those collected at the badland test plots, Šterna (U1) – 4 samples, Boljun (U2) – 6 samples, Sv. Donat (U2) – 2 samples, Botonega (U4) – 1 sample.

These carbonate data complement the durability test results and provide context for the interpretation of lithological controls on weathering sensitivity and denudation.

3.6. Marl durability

The most widely used laboratory method for determining the durability of clay-rich rocks is the slake durability test, for which the International Society of Rock Mechanics issued a recommendation in 1977 (ISRM, 1977). However, this test has often been criticized for its limited number of two wetting–drying cycles (GAMBLE, 1971; TAYLOR, 1988; GOKCEOGLU & AKSOY, 2000), which may not provide sufficient resolution for weak, clay-rich marls, as many specimens show little or no change during the initial cycles.

To achieve greater sensitivity and better simulate repeated wetting–drying and freeze–thaw conditions, modified 20-cycle protocols were implemented in this study (Table 2). Conceptually, the procedure follows the cyclic approach of the former JUS Regulation (1982) for freeze resistance, but replaces endpoint visual assessment with per-cycle mass-loss measurements. After each cycle, fragments smaller than 1 cm were removed and treated as disintegrated material (Fig. 9). The 1 cm threshold is not a standard value, but an empirically selected operational criterion applied consistently throughout the tests to distinguish relatively intact fragments from finer breakdown products that are more readily available for subsequent gravitational or surface-water transport under field conditions. This procedure provided a consistent basis for comparing disintegration rates among samples and EG units.

Each test began with 40–60 g of air-dry fragments. After every drying phase, fragments smaller than 1 cm were removed (Fig. 9) and the remaining mass (bigger than 1 cm) was weighed to calculate per-cycle and cumulative mass loss.

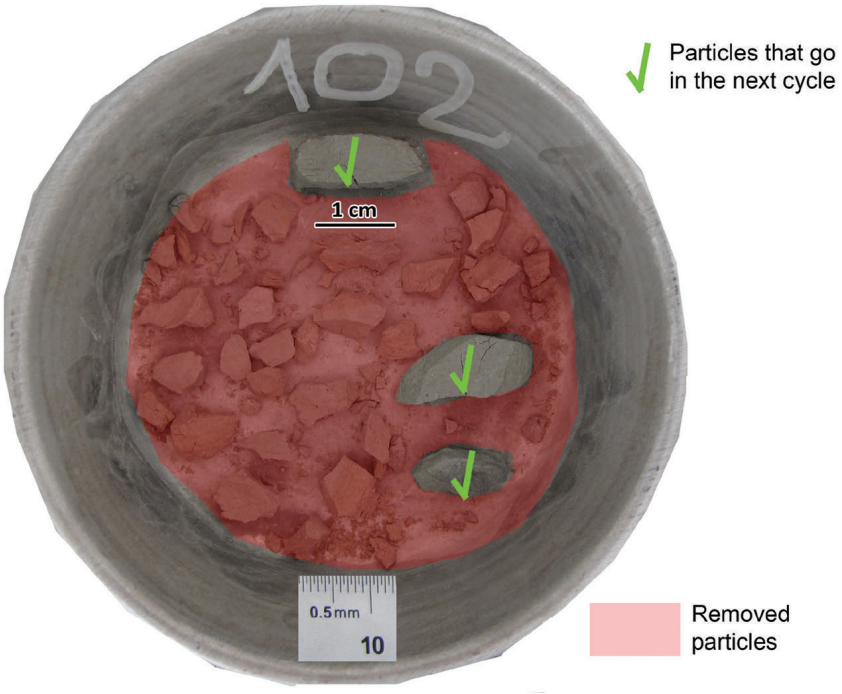


Figure 9. Removal of particles smaller than 1 cm during the durability assessment.

Table 2. Durability assessment: Testing conditions and number of cycles for each test.

Protocol	Process	Conditions	Process duration	1 cycle duration	Number of cycles
DWF	Drying	105 °C	16 h	24 h	20
	Wetting	Distilled water	2.5 h		
	Freezing	-18 °C	3.5 h		
DW	Drying	105 °C	16 h		20
	Wetting	Distilled water	2.5 h		

For comparability across protocols and EG units, the mass loss of each specimen was converted into a durability score, assigned on an ordinal scale from 1 (most durable) to 6 (least durable), as follows:

- 1: completed all 20 cycles with <10 % cumulative mass loss,
- 2: completed all 20 cycles with ≥10 % cumulative mass loss or disintegrated during cycles 17–20,
- 3: disintegrated during cycles 13–16,
- 4: disintegrated during cycles 9–12,
- 5: disintegrated during cycles 5–8,
- 6: disintegrated during cycles 1–4.

The durability scores obtained in this way provide a numerically tractable index of disintegration rate and support subsequent comparisons with unit-level denudation patterns.

To capture the weathering sensitivity of clay-rich marls in Grey Istria, 63 field samples were prepared and organized according to the EG unit framework (Table 3): U1 – 17 samples, U2 – 36 samples, U4 – 10 samples. These 63 samples also include those collected at the badland test plots, Šterna (U1) – 6 DW samples, Boljun and Sv. Donat (U2) – 11 DW samples, and Botonega (U4) – 1 sample for both DWF and DW protocols.

3.7. Photogrammetric and profilometers denudation measurement

Denudation rates on badland test plots were quantified using terrestrial photogrammetry (analogue and digital), complemented by profilometer readings. Stereo image pairs captured the micro-topography, enabling detection of elevation changes and calculation of average lowering rates between repeated survey epochs.

To ensure inter-epoch comparability, a local (relative) coordinate system was established on each test plot by defined ground control points. Five to six pins were anchored in competent, stable substrate and their positions were precisely measured with a Leica TCR 705 total station. This configuration allowed consistent resection and co-registration of stereo models between epochs, effectively removing differences due to camera position/orientation and providing a stable geometric basis for change detection.

Two types of cameras were used for photogrammetric measurements:

- analogue metric camera (WILD P31) for larger parcels of app. 95–175 m² (Fig. 10a),
- digital cameras (6 MP FUJI FinePix S2 Pro and 12 MP NIKON D90) for smaller parcels of app. 3.5–16 m² (Figure 10B).

Table 3. Number of specimens per EG unit used in the DWF and DW durability protocols.

EG unit	Number of samples	DWF protocol specimens		DW protocol specimens	
		Field sampling	Badland test plot	Field sampling	Badland test plot
U1	17	11	0	11	6
U2	36	25	0	17	11
U4	10	9	1	9	1
Total	63	45	1	37	18

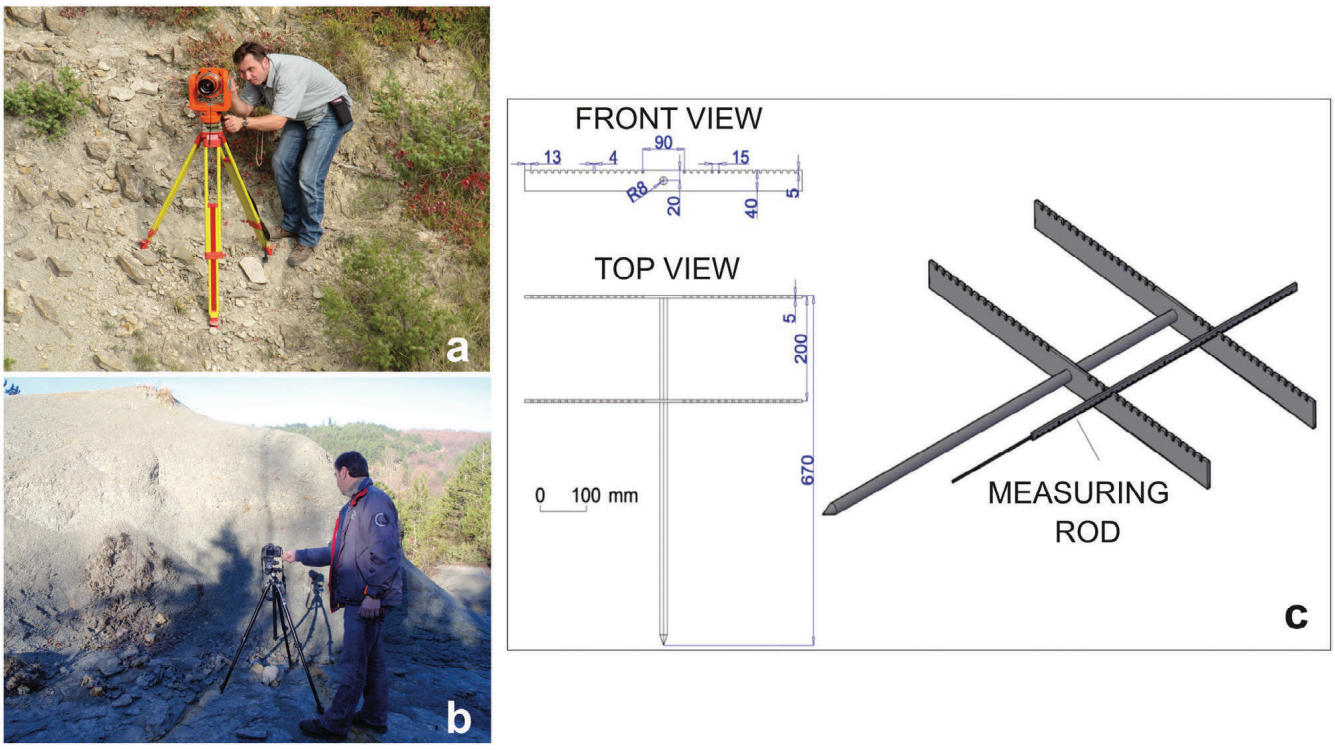


Figure 10. Denudation measurements at badland test plots: (**a**) Analogue photogrammetry; (**b**) Digital photogrammetry; (**c**) Profilometer device.

Stereo image sets were acquired with appropriate baseline and convergence, processed to generate surface models, and differenced across epochs to produce elevation-change maps and parcel-average denudation rates.

Internal photogrammetric precision was evaluated from control-point and tie-point residuals within the local frame. For digital imagery, pixel size provided a practical lower boundary on spatial resolution; for the analogue system, manufacturer specifications and internal residuals were used to characterise measurement error. These internal errors (in a range from app. 1 to 6 mm) quantify the geometric precision of the photogrammetric solution, but do not include true surface changes.

Profilometers provided complementary, low-cost denudation measurements. Various types of profilometers are used worldwide (MCCOOL et al., 1981; RAMIREZ, 1988; HUDSON, 1993), The device used in this study consists of two elongated flat iron bars connected by a central pin (Fig. 10c), allowing reproducible micro-relief readings. Whenever possible, profilometers were placed in inaccessible locations using climbing equipment to prevent damage or vandalism.

4. RESULTS

4.1. GSI distribution across engineering--geomorphological units

GSI ranges were assessed at 55 field observation points and assigned to the corresponding EG units. The resulting distributions are presented in Figure 11 and summarized in Table 4.

U1 shows the largest variability in both structural type and GSI, spanning Types II–VI (dominantly Type VI and Type II, with transitional II–VI). GSI values range from 30–40 up to 55–65, indicating spatially heterogeneous conditions within the unit. This spread likely reflects local differences in lithological alternation and the degree of disturbance and weathering along the slopes where U1 occurs.

Table 4. Summary of GSI estimates by EG unit (from field observation points).

EG unit	No. of points	Dominant GSI structural types	Overall GSI range (min–max)	Most frequent GSI range(s)
U1	12	VI (6), II (4), II–VI (2)	30–65	35–45 (5), 55–65 (4)
U2	31	IV (15), V (8), IV–V (5)	35–60	45–55 (14), 40–50 (6), 43–53 (6)
U4	12	II (12)	45–70	55–65 (10)

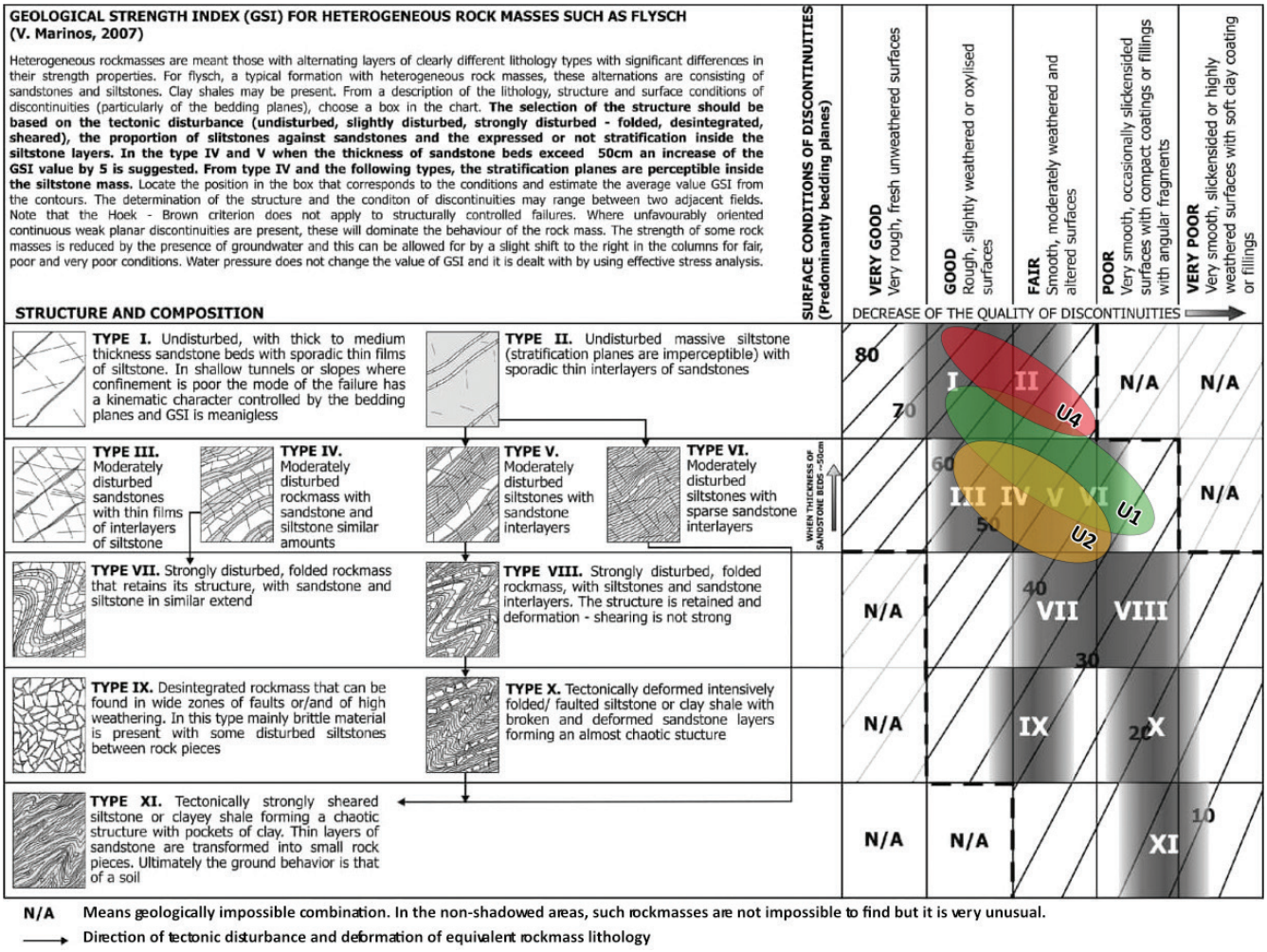


Figure 11. Distribution of GSI values per EG unit.

U2 is characterized mainly by moderately disturbed heterogeneous flysch and plots predominantly within Types IV–V (with minor Type III, V–VI and VII occurrences). The GSI ranges are concentrated around 45–55 (14/31 points), followed by 40–50 and 43–53 (6/31 each), indicating a moderate rock mass quality and a relatively limited spread. The position of U2 on the chart suggests that rock mass behaviour is controlled by the combined effect of heterogeneity (alternation of lithologies) and moderate tectonic disturbance and/or weathering.

U3 (megabeds) was not formally classified using the MARINOS (2010) GSI scheme because its thick and highly competent beds fall outside the weak and complex rock-mass range for which the applied chart was developed. Nevertheless, based on their intact to blocky structure and generally favourable discontinuity conditions, these rock masses would be expected to occupy the upper part of the GSI range, most likely above 65. This interpretation is qualitative and is not included in the statistical comparison of GSI values among the EG units.

U4 plots dominantly within Type II (undisturbed, massive siltstone-marl with sporadic thin sandstone interlayers) and occupies the upper part of the chart. Field estimates cluster tightly around GSI 55–65 (10/12 points), with occasional values of 45–55 and 60–70. This narrow range indicates a comparatively more intact and less disturbed rock mass fabric, with discontinuities sparse to practically absent, which distinguishes U4 from the remaining units.

The predominant occurrence of Type II and Type VI in U4 and U1 indicates comparatively more homogeneous rock masses, in which slope degradation is suggested to be dominated by sheet erosion and surface wash. In contrast, U2 plots mainly within Types III–V, reflect a heterogeneous flysch fabric with alternating competent and incompetent layers; competent beds can buttress and locally stabilise steeper slopes, but they also promote rockfall-type processes (e.g., planar or wedge failure and toppling) through bed-controlled detachment. Consequently, the GSI-based differentiation among units suggests not only differences in rock-mass quality but also systematic contrasts in the prevailing chain of slope processes.

4.2. $CaCO_3$ content and marl durability scores

To test whether the applied unit subdivision is meaningful from an EG perspective, marl durability was quantified across the predefined units using laboratory durability tests and combined with calcimetry data ($CaCO_3$ content, %). This joint dataset enables assessment of lithological control on material breakdown and establishes the material context for the denudation patterns reported in Section 4.3.

4.2.1. $CaCO_3$ content

Across the study area, $CaCO_3$ content differs systematically among the EG units, reflecting their sedimentological characteristics. Unit mean values show a clear separation (Fig. 12): (i) U4 exhibits the highest $CaCO_3$ content (range from 59.1 % to 78.9 %), consistent with the presence of more competent carbonate material within the marls; (ii) U1 is intermediate (range from 46.6 % to 73.7 %); and (iii) U2 shows the lowest $CaCO_3$ content (range from 23.4 % to 59.0 %), reflecting the high clay proportion within its non-competent member.

On the test plots, these contrasts are also evident: samples taken from Šterna (U1) and Botonega (U4) show high $CaCO_3$ content, whereas those taken from Sv. Donat (U2) and Boljun (U2) display lower average values.

4.2.2. Durability

Under the DWF protocol, unit mean values show a clear separation between U4 and the other units (Fig. 13). U4 exhibits the lowest scores (i.e., highest durability), with values restricted to a narrow range (≈ 1–2), whereas U1 and U2 yield higher scores and broader ranges (U1 ≈ 4–6; U2 ≈ 2–6). In addition to mean differences, the dispersion is diagnostic:

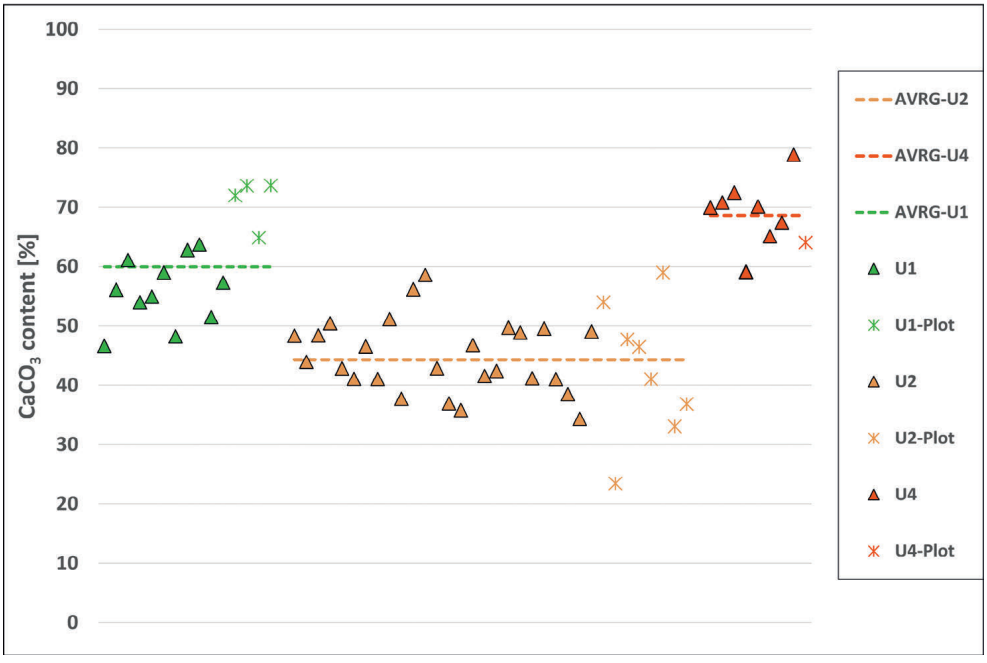


Figure 12. Distribution of $CaCO_3$ content (%) across EG units (U1, U2, U4).

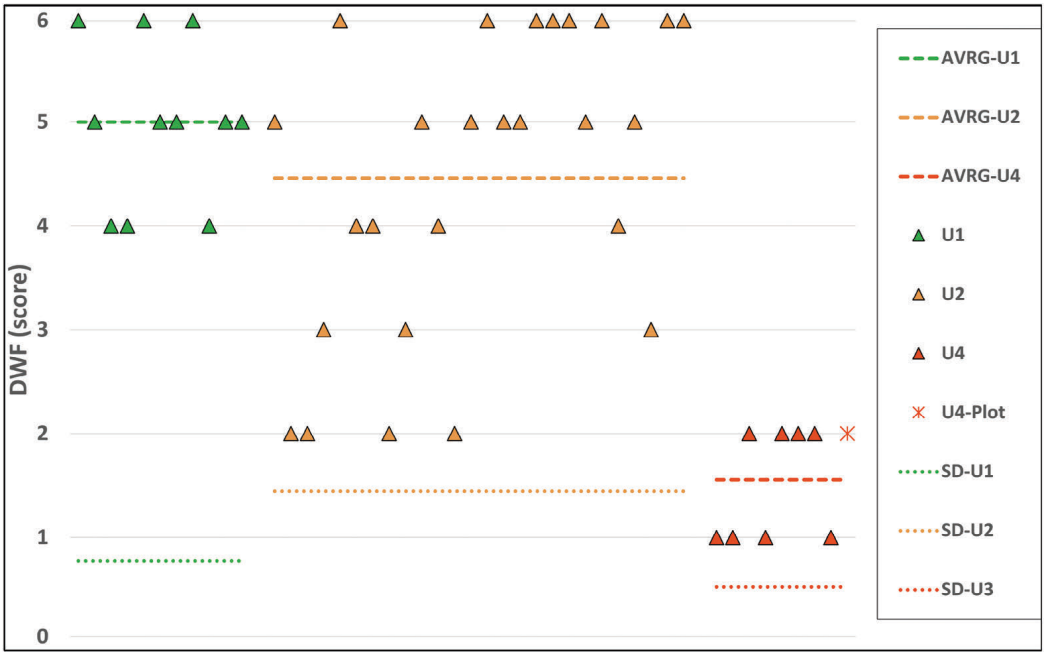


Figure 13. Distribution of DWF durability scores across EG units (AVRG = average; SD = standard deviation).

standard deviation (SD) is highest in U2, followed by U1, and is lowest in U4 (Fig. 13). This indicates that U2 non-competent materials show the greatest variability in freeze–thaw–assisted breakdown, while U4 behaves most uniformly.

When freeze–thaw is removed, the DW protocol yields the most consistent unit ranking (Fig. 14). U4 remains the most durable, with low scores (≈ 1–2), U1 is intermediate (≈ 1–5), and U2 is the least durable, showing the highest mean scores and the widest range (≈ 1–6). The dispersion hierarchy persists in the same sense as for DWF SD(U2) > SD(U1) > SD(U4) supporting the interpretation that variability is greatest in U2 and lowest in U4. This spread likely reflects sampling across different weathering zones as well as intrinsic heterogeneity.

Without freeze–thaw stress, carbonate-rich U4 maintains consistently low durability scores, U1 occupies an intermediate position, and carbonate-poor U2 generally exhibits higher scores. A general inverse relationship between $CaCO_3$ content and durability score is therefore observed under DW conditions, whereas the DWF results indicate that additional controls beyond carbonate content influence durability. This suggests that $CaCO_3$ content alone cannot fully explain durability variability across the EG units.

Calcimetry shows a clear unit separation in carbonate content, with $CaCO_3$ content highest in U4, intermediate in U1, and lowest in U2 (Fig. 8). In the DW test, this ordering aligns with the expected inverse $CaCO_3$–durability relationship

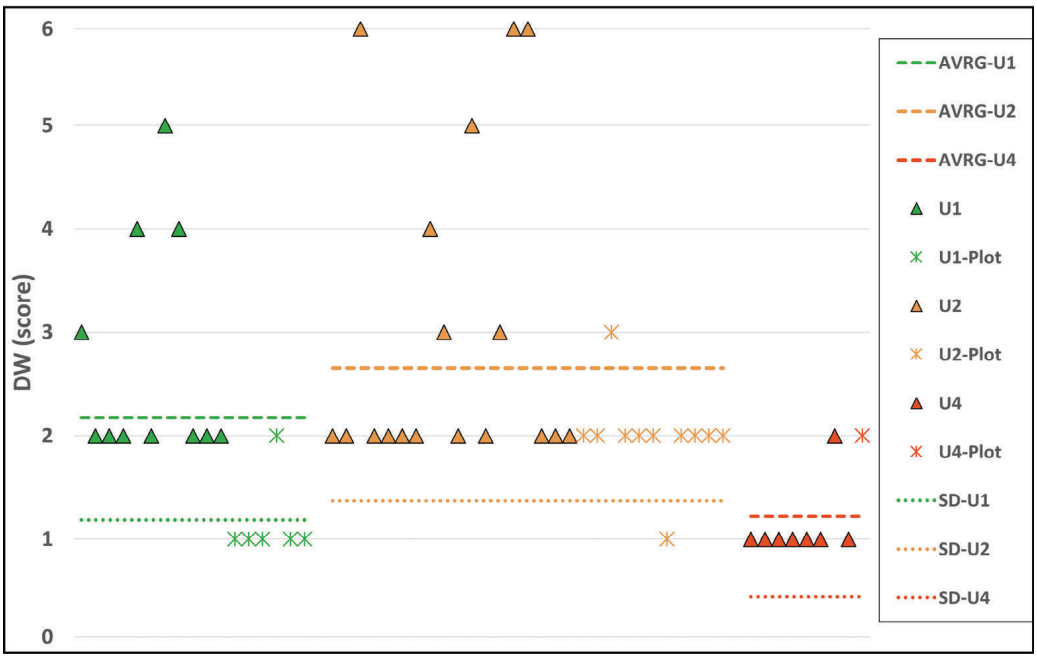


Figure 14. Distribution of DW durability scores across EG units (AVRG = average; SD = standard deviation).

(higher $CaCO_3$ ↔ lower durability scores). Without freeze–thaw stress, Carbonate-rich U4 maintains consistently low scores, U1 occupies an intermediate position, and carbonate-poor U2 clusters at higher scores. Under DWF, however, the carbonate signal is only partly expressed: although U4 remains the most durable (consistent with its high $CaCO_3$), the relative ordering of U1 and U2 reverses, with U2 showing lower (better) mean DWF scores than U1. This may indicate that freeze–thaw introduces additional controls beyond carbonate content alone, potentially related to differences in material fabric, microfracturing, moisture accessibility, and/or the inclusion of specimens from different weathering zones. The implications of this non-monotonic response are addressed in Subsection 5.1.

4.2.3. Badland test plots

To directly connect material behaviour with measured surface lowering (Subsection 4.3.), plot-specific durability and $CaCO_3$ are summarized as follows:

- Šterna (U1): DW tests indicate high durability on plot material, consistent with high $CaCO_3$,
- Sv. Donat (U2): DW tests and $CaCO_3$ confirm lower durability and lower carbonate content,
- Boljun (U2): DW tests indicate lower durability; $CaCO_3$ is higher than at Sv. Donat but remains below U1/U4,
- Botonega (U4): paired DWF and DW results together with $CaCO_3$ indicate durable, carbonate-rich material.

These plot-specific material fingerprints provide the basis for interpreting differences in denudation rates among badland test sites, beyond the influence of morphology alone.

4.3. Denudation rates on badland test plots

This section addresses the third objective of this study – to quantify denudation rates on representative badland plots – and examines whether the lithological control, identified in Subsection 4.2. ($CaCO_3$ content and marl durability scores), correspond to measurable differences in surface lowering. Denudation results from four badland test plots located in different EG units were analyzed and total denudation over the observation period was compared with corresponding average annual rates (Fig. 15).

If higher $CaCO_3$ content corresponds to lower durability scores (e.g., higher durability) and if the SD hierarchy (U2 > U1 > U4) partly reflects sampling across weathering zones, then U2 badland test plots would be expected to record higher denudation, U4 the lowest, and U1 intermediate – subject to local morphometry and flow contact.

4.3.1. Šterna – U1

Digital photogrammetry shows a total lowering of ≈ 3.3 cm over the observation period, i.e. ≈ 1.4 cm/yr. Combined with high $CaCO_3$ and low DW, Šterna exemplifies the intermediate behaviour expected for U1. Denudation is noticeable but not clearly lower than on U2 badland plots. Local slope of the test plot is gentle to moderate (≈ 18–40°) and limited channel–toe contact favours a sheet-dominated denudation type.

4.3.2. Sv. Donat – U2

Digital, analogue, and profilometer series consistently show the highest denudation among all badland testing plots, in a total of ≈ 4.5–7.0 cm over the measurement period and annually of ≈ 2.0–4.4 cm/yr, depending on method/period. This matches the lower $CaCO_3$ and higher durability scores measured in U2 materials. Slopes of the test plot are very steep (≈ 50–80°, locally 64–68°), and the against-dip wall experiences frequent channel–toe contact, which concentrates stream power and sustains curtain-type bare strips.

4.3.3. Boljun – U2

Patterns closely mirror those at Sv. Donat, with high denudation rates, in totals of ≈ 4.3–9.0 cm over the measurement period and annually of ≈ 3.2–4.2 cm/yr, consistent with the material properties characteristic of U2. Steep sidewalls of the test plot (≈ 40–70°, typically 55–60°) and efficient evacuation of fines maintain persistent bare surfaces despite partial sandstone armouring.

4.3.4. Botonega – U4

Digital photogrammetry and profilometry record the lowest denudation among all badland test plots, in totals of ≈ 0.8–1.7

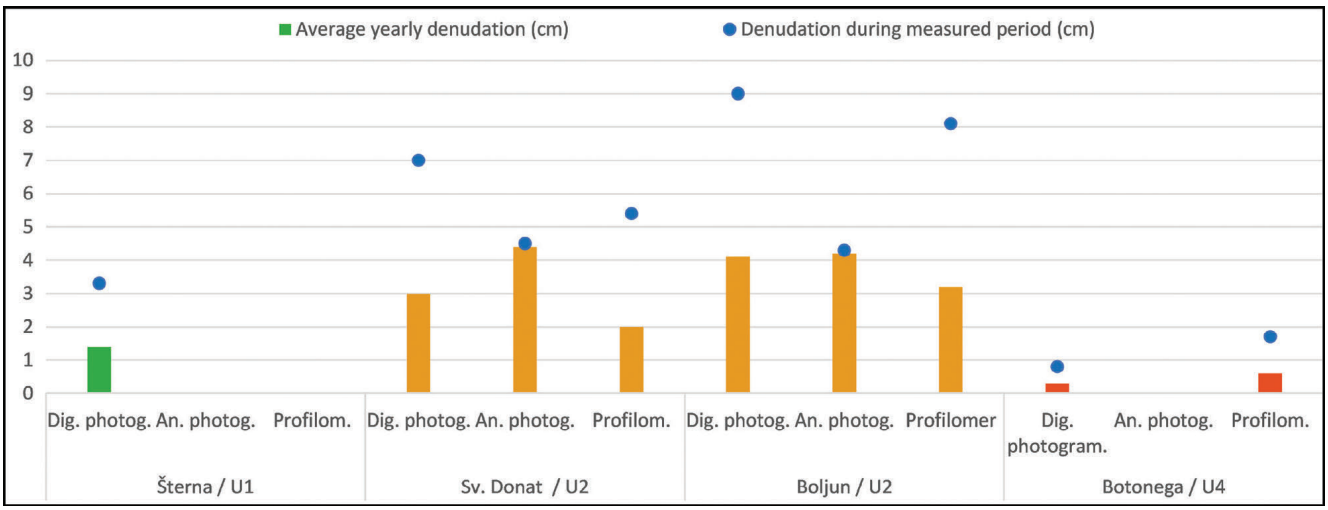


Figure 15. Average denudation rates on test plots measured with different techniques across different EG units

cm over the measurement period and annually of ≈ 0.3–0.6 cm/yr. This is fully consistent with high $CaCO_3$ and low durability scores of U4, as well as with its gentler slopes (≈ 35–39°) and weaker flow focusing along the badland plot.

Results from all badland test plots confirm the following statements:

- material control appears to be reflected in the field: denudation ranks as U2 > U1 > U4, which mirrors the trends in $CaCO_3$ content and marl durability,
- morphometry modulates magnitude: steep against-dip walls and frequent channel–toe contact (Sv. Donat, Boljun) amplify U2's susceptibility, while gentler slopes and limited contact (Šterna, Botonega) supress denudation even where material is weaker than in U4,
- denudation measurement methods agreement is strong: where two or three methods overlap, they yield consistent relative ranking. Discrepancies in absolute magnitudes reflect differences in spatial scale and observation period (e.g., analogue campaigns spanning ≈ 1 yr vs. multi-year digital/profilometer series).

These results also indicate that laboratory durability and present-day denudation should not be interpreted as having a simple one-to-one relationship. Lower material durability reflects a greater susceptibility to breakdown, but the resulting denudation rate also depends on local slope geometry, the efficiency of sediment evacuation, and the frequency of channel–toe contact.

5. DISCUSSION

5.1. Engineering-geomorphological units

The results presented here provide consistent support for the delineation of the proposed preliminary EG units in the terrain of Grey Istria. Their validity and practical utility are supported by four complementary lines of evidence: (i) field-based rock-mass characterization using GSI; (ii) calcimetry ($CaCO_3$ content) as a proxy for the relative clay-rich vs. carbonate-rich composition; (iii) laboratory durability behaviour under extended cyclic DWF/DW experiments; and (iv) plot-scale denudation measurements. In combination, these datasets converge on a consistent pattern: materials richer in clay minerals, with lower $CaCO_3$ content exhibit lower durability and higher denudation, whereas $CaCO_3$-rich marls behave more durably and tend to show lower retreat under comparable morphometric settings. Taken together, our results indicate that lithological composition (expressed through the clay–carbonate balance and associated durability) strongly influences the denudation regime in Grey Istria, consistent with interpretations reported from other badland and marl–flysch settings (KASANIN-GRUBIN & BRYAN, 2007; BRYAN & YAIR, 1982).

Still, as flagged in Section 4.2.2., the DWF series shows a partial departure from the $CaCO_3$-guided ordering, where U4 remains most durable, but U1 and U2 reverse, with U2 attaining better (lower-loss) mean DWF scores than U1. The observed DWF non-linearity was interpreted as evidence that freeze–thaw introduces controls beyond carbonate content alone, notably (a) pore architecture and fabric (pore-size distribution, microcracking, bedding-parallel anisotropy), which govern ice lensing and hydraulic pressure; (b) moisture accessibility and preconditioning (degree/time to saturation during the test); and (c) weathering-zone mix in the sampled material, with near-surface, more altered U1 specimens potentially contributing to lower DWF durability. In other words, while $CaCO_3$ tracks DW well, DWF is more sensitive to fabric and saturation kinetics, which can invert U1–U2 at the laboratory scale without contradicting the field reality that U2 badlands denude faster where toe scour is frequent. Practically, this non-linearity argues for reporting durability by weathering zone and for standardised saturation pre-conditioning; selectively adding porosity/mercury intrusion or XRD/XRF on a small subset may help separate lithological from alteration effects.

5.1.1. Unit-scale synthesis

In light of the observed links between material indicators ($CaCO_3$ / clay-richness), rock-mass fabric (GSI), laboratory behaviour (durability), and field response (denudation), the characteristic behaviour of the principal EG units can be summarized as follows:

- U4 (more intact fabric; higher GSI): Tends to behave as the more durable weak-rock unit. Denudation is generally lower under comparable morphometric conditions, and erosion is more likely to proceed via sheetwash-dominated lowering, reflecting the unit's relatively homogeneous and intact rock-mass fabric,
- U2 (moderately disturbed, heterogeneous fabric; moderate GSI): Commonly exhibits the least favourable durability–denudation combination in the field. Denudation on U2 badland surfaces is typically more spatially variable than in U4, reflecting pronounced lithological heterogeneity. The alternation of competent beds (mainly sandstone) and incompetent beds (mainly marl), together with discontinuities, favours rapid breakdown. Raveling and small slides are more frequent where the slope toe is recurrently undercut by channel–toe contact (GULAM et al., 2014). In the laboratory, DW follows the $CaCO_3$ trend, whereas DWF can rate U2 above U1, consistent with freeze–thaw sensitivity to fabric and saturation rather than composition alone,
- U1 (highly variable fabric; wide GSI span): Presents the most spatially heterogeneous response. Denudation type and magnitude can shift markedly over short distances as the balance between disturbance/weathering, local alternation, and slope setting changes. The lower-than-expected DWF durability scores of U1 relative to U2 may reflect differences in weathering state and pore-structure sensitivity to freeze–thaw damage; however, these controls were not directly measured in this study and should therefore be regarded as possible explanations,
- U3 (competent carbonate bodies / megabed-scale competent members): Rarely host active badland slopes, but they organise the geomorphological system by setting local base levels and knickpoints—often expressed as distinct erosion steps—thereby influencing where adjacent weaker units can sustain erosion and continued

retreat (GULAM, 2012; PETRINJAK et al., 2021). This observation is qualitative here and will be quantified in forthcoming work on morphometric characteristics.

In practical terms, the proposed EG units provide a workable framework for large-scale EG mapping and spatial discretization of the Grey Istria flysch. Because the units are defined to separate domains that differ in lithology, mineralogical (clay–carbonate) signature, and mechanical behaviour, they offer a consistent basis for organising the landscape into mappable entities with contrasting degradational response. As such, this classification represents a useful starting point for future geomorphological and morphometric analyses, where unit-based stratification can support clearer spatial attribution and comparison of denudation patterns across the study area.

5.2. Appraisal of applied methods

5.2.1. Marl durability

The extended-cycle protocol (≈ 20 cycles) proved effective because it expands the dynamic range and separates samples at different alteration states, consistent with earlier critiques that the standard two-cycle slake durability test often lacks sufficient resolution for weak, clay-rich materials (GAMBLE, 1971; TAYLOR, 1988; GOKCEOGLU & AKSOY, 2000) This explains the larger within-unit SD, because the method is sensitive to intra-unit heterogeneity (lithological and weathering-zone variability), which is precisely the information needed to understand why the same EG unit can host both fast and slow retreat. The added resolution facilitated the linking of durability ranks to denudation type and rate on representative badland plots. To avoid conflating lithology with alteration state, future sampling campaigns should explicitly control for weathering zones, since specimens from different depths or alteration states systematically differ in durability even within the same EG unit.

5.2.2. Sampling and weathering zones

Sample numbers are uneven among units and sites, and some samples originate from different weathering depths. In addition, samples collected from road-cuts may differ from those obtained from natural badland exposures because of differences in exposure history, drainage conditions, and disturbance related to excavation. This represents an additional source of uncertainty when comparing durability results among sampling locations. Because alteration state reduces durability, cross-unit comparisons must acknowledge this source of scatter.

The standard deviation hierarchy indicates that the tested materials span different weathering states. Consequently, a simple one-to-one mapping between a single durability value and a single denudation rate is unwarranted without considering morphometric context, (slope angle, slope geometry, and the frequency and duration of channel–toe contact).

A key implication is that lower laboratory durability does not always correspond to higher present-day denudation. Specimens from advanced weathering zones near the surface may appear less durable because they have already undergone many wetting–drying and freeze–thaw cycles; yet, if toe scour is intermittent, their current denudation may remain low. The decisive control in the exogenetic process chain is the frequency of contact between the erosive channel and the badland toe; without recurrent toe scour, even weak marls can exhibit modest short-term retreat. Therefore, interpreting durability–denudation relationships requires explicit consideration of slope geometry, morphometric setting, and toe-contact dynamics.

5.2.3. Calcimetry

Calcimetry provides a quick, low-cost estimate of $CaCO_3$ content (HEAD, 1982). In the presented dataset, $CaCO_3$ content shows a general trend that contributes to the differentiation of the marl-dominated EG units: U2 has the lowest $CaCO_3$ content, indicating a higher proportion of non-carbonate components, and generally exhibits lower durability and higher denudation than U1 and U4. Thus, calcimetry offers an independent, scalable check that strengthens the unit-based interpretation and helps resolve within-unit variability. Thereby, near-surface decalcification can depress $CaCO_3$ irrespective of primary lithology and calcimetry does not resolve clay mineralogy or cementation. Therefore in this study calcimetry is used alongside durability tests and it is recommended that it is calibrated on a small XRD/XRF subset in future studies.

5.2.4. Photogrammetry

Field results confirm the high potential for denudation monitoring in central Istria. Digital photogrammetry is operationally superior in terms of cost, flexibility, and scalability, even if its nominal precision can be slightly lower than analog approaches (GULAM et al., 2018). In practice, higher repeatability and greater efficiency make it the preferred choice for monitoring networks. Analog systems can reach excellent accuracies but remain impractical due to costly hardware and time-intensive workflows. Photogrammetry on texture-poor surfaces (e.g., very uniform marls) can limit point matching, and short monitoring windows may capture episodic rather than representative longer-term behaviour. Multi-scale and multi-sensor strategies, combining ground-based or pole-mounted imagery, UAV surveys (RGB and/or LiDAR), and terrestrial laser scanning, can mitigate these limitations, but they require rigorous co-registration and cross-calibration across sensors and epochs, as well as explicit treatment of registration uncertainty in DEM/DoD-based change detection (NEUGIRG et al., 2016; WILKINSON et al., 2016; LETORTU et al., 2018; BERTIN et al., 2022).

5.2.5. Profilometers

Profilometers represent a robust, low-cost auxiliary tool with limited spatial coverage (profiles on the order of a few decimetres). They are useful for first-order annual retreat estimates and for cross-checking photogrammetric trends, but are not a substitute for avide-area surface change detection.

5.3. Future work and open questions

Although the results of this study confirmed the role of material properties in controlling denudation, some open questions and opportunities for further research still remain.

Further work can deepen understanding of the temporal and spatial variability of processes, improve denudation measurement methodologies, and enable more accurate predictions of badland dynamics. This section outlines the directions for future investigations:

• LiDAR-driven morphometric fingerprints of badlands in central Istria

By leveraging the 2024 national LiDAR release along with targeted drone-LiDAR acquisitions, high-resolution DEMs and morphometric indices such as slope, curvature, planform metrics, confinement, stream order, and local relief can be derived (WOOD, 1996; WILSON & GALLANT, 2000; PIKE et al., 2008). These data will allow quantification of unit-specific morphometric envelopes, testing of thresholds for toe-contact likelihood, and construction of a predictive framework that links EG units with morphometry, which can subsequently be used for susceptibility mapping. The expected outcome is a reproducible workflow and a comprehensive morphometric atlas associated with EG units.

• Denudation analysis from nine badland test plots

The multi-sensor record, integrating drone RGB/LiDAR, tripod RGB, and terrestrial laser data across different scales, will be systematically analyzed alongside rainfall and mini-meteorological station records to quantify denudation from single events up to the seasonal scale (NEUGIRG et al., 2016; CHEN, 2026). This will enable isolation of process partitioning between sheetwash and raveling/slides for each unit and slope class, quantification of climate–denudation relationships, and evaluation of the persistence of toe scour under varying antecedent moisture conditions. Deliverables will include cross-calibrated DEMs of difference and unit-specific denudation response curves (WHEATON et al., 2010; WILLIAMS, 2012).

• Using durability to map weathering zones

Refining the durability protocol, including cycle design, fragment handling, and statistical treatment, and explicitly linking results to field-mapped weathering zones will allow marls to be partitioned into durability classes per unit. When integrated with local morphometry, these classes will enable first-order predictions of average annual sidewall retreat at sites of interest. The ultimate aim is to develop an EG-aware operational framework that estimates denudation from the combination of durability class, morphometry, and toe-contact frequency without requiring long-term monitoring.

6. CONCLUSION

The subdivision of geological members in Grey Istria into EG units is conceptually meaningful and supported by the material properties and geomorphological data presented here. Laboratory durability tests, calcimetry, GSI-based rock-mass characterization, and denudation measurements from four pilot badland plots consistently show that Units U1 (Massive Globigerina marls), U2 (Marl–sandstone alternation), U3 (Megabeds), and U4 (Thick marl intervals above the Megabeds) differ in their intrinsic lithological and mineralogical properties which leads to distinct EG behaviour. These differences exert a first-order control on badland activity and sediment production within the flysch terrain of Grey Istria.

(1) Marl durability as a discriminator among units

Across the applied weathering-test protocols (DWF and DW), durability results consistently separate the EG units, with U2 showing the lowest resistance to disintegration and U4 the highest. Freeze–thaw cycling increases absolute degradation and locally modifies relative responses, but does not obscure the dominant contrasts between units. This indicates that durability differences primarily reflect intrinsic material properties rather than solely the degree of surface weathering.

(2) Durability variability (standard deviation) is itself diagnostic

The consistent pattern SD(U2) > SD(U1) > SD(U4) reflects the strong internal heterogeneity of U2 and highlights the influence of sampling across different weathering zones. These results underline that durability results must be interpreted with explicit consideration of sampling depth and weathering context.

(3) Calcimetry reflects the lithological control on durability

$CaCO_3$ content clearly separates the units (U4 highest, U1 intermediate, and U2 lowest) and shows an inverse relationship with the durability score, with higher $CaCO_3$ corresponding to higher material resistance. This relationship is expressed both at the unit scale and at the test-plot scale (Šterna and Botonega with higher $CaCO_3$ and higher durability vs. Sv. Donat and Boljun with lower $CaCO_3$ and lower durability), confirming the primary role of lithology in controlling mechanical weathering behaviour.

(4) GSI complements durability by capturing rock-mass structure

While durability reflects the intrinsic resistance of marl to mechanical breakdown, GSI characterizes the structural condition and degree of disturbance of the rock mass. The distribution of GSI values across the EG units is consistent with their lithological composition and degree of internal heterogeneity, particularly highlighting the structurally complex nature of U2. Together, durability and GSI provide a more complete description of material behaviour than either parameter alone.

(5) Denudation measurements support a material-based control framework

The lowest annual denudation rates were measured at Botonega (U4) and Šterna (U1) (0.3–0.6 cm/yr and ≈ 1.4 cm/yr), corresponding to units characterized by higher durability, higher $CaCO_3$ content, and more favourable GSI ranges. In contrast, the highest denudation rates (2–4.4 cm/yr) were recorded at Sv. Donat and Boljun, sites developed within U2, where low durability, low carbonate content, and structurally unfavourable rock-mass conditions coincide. The denudation hierarchy therefore broadly mirrors the combined durability–GSI framework at unit scale, confirming that lithology and rock-mass structure together govern badland denudation intensity in Grey Istria.

Practical implications arise directly from these findings:

(i) For large-scale EG mapping and land management, U2 domains should be considered the most erosion-prone due to

the combined effect of low durability and unfavourable rock-mass structure,

(ii) Future studies should integrate durability testing, calcimetry, and GSI assessment, with controlled sampling across weathering zones, to reduce interpretive ambiguity and improve the predictive value of EG unit mapping.

Overall, the study validates the engineering-geomorphological subdivision of the Grey Istria flysch and demonstrates that material properties, particularly durability, carbonate content, and rock-mass structure expressed by GSI, are key controls on badland denudation patterns. This integrated framework provides a solid basis for future research and for the application of engineering–geomorphological units in hazard assessment, land-use planning, and erosion management within the flysch terrain.

ACKNOWLEDGEMENT

This paper was supported by the internal research project "Dynamics of Istrian badlands: from sample to catchment (DONA)" at the Croatian Geological Survey, funded by the European Union – NextGenerationEU under the National Recovery and Resilience Plan 2021–2026.

References

BABIĆ, L. & ZUPANIČ, J. (1996): Coastal dinaric flysch belt: paleotransport model for the Pazin Basin, and the role of a foreland uplift.– Natura Croatica, 5, 317–327.

BABIĆ, LJ., HERNITZ-KUČENJAK, M., ĆORIĆ, S. & ZUPANIČ, J. (2007): The Middle Eocene age of the supposed Late Oligocene sediments in the flysch of the Pazin Basin (Istria, Outer Dinarides).– Natura Croatica, 16/2, 83–103.

BERGANT, S., TIŠLJAR, J. & ŠPARICA, M. (2003): Eocene Carbonates and Flysch Deposits of the Pazin Basin.– In: VLAHOVIĆ, I. & TIŠLJAR, J. (eds.): Field Trip Guidebook.– 22nd IAS Meeting of Sedimentology, Opatija, September 17–19, Croatian Geological Survey, 57–63.

BERGANT, S., MATIČEC, D., FUČEK, L., PALENIK, D., KORBAR, T., ŠPARICA, M., KOCH, G., GALOVIĆ, I. & PRTOLJAN, B. (2020): Osnovna geološka karta RH 1:50 000, list Rovinj L 2 [*Basic Geological Map of the Republic of Croatia 1:50 000, Rovinj sheet L 2* – in Croatian].– Department of Geology, Croatian Geological Survey, Zagreb.

BERTIN, S., JAUD, M. & DELACOURT, C. (2022): Assessing DEM quality and minimizing registration error in repeated geomorphic surveys with multi-temporal ground truths of invariant features: Application to a long-term dataset of beach topography and nearshore bathymetry.– Earth Surface Processes and Landforms, 47, 2950–2971. https://doi.org/10.1002/ESP.5436

BOSTJANČIĆ, I., GULAM, V., FRANGEN, T. & HEĆEJ, N. (2022): Relation between relief and Badland spatial distribution in the Paleogene Pazin Basin, Croatia.– Journal of Maps, 19/1. https://doi.org/10.1080/17445647.2022.2163196

BOUMA, N.A. & IMESON, A.C. (2000): Investigation of relationships between measured field indicators and erosion processes on badland surfaces at Petrer, Spain.– Catena 40/2, 147–171. https://doi.org/10.1016/S0341-8162(99)00046-6

BRYAN, R.B. & HARVEY, L.E. (1985): Observations on the geomorphic significance of tunnel erosion in a semi-arid ephemeral drainage system.– Geografiska Annaler: Series A, Physical Geography, 67/3–4, 257–272. https://doi.org/10.1080/04353676.1985.11880151

BRYAN, R.B. & YAIR, A. (1982): Perspectives on studies of badland geomorphology.– In: BRYAN, R.B. & YAIR, A. (eds.): Badland geomorphology and piping. GeoBooks, Norwich, 1–12.

CHEN, Y.-C. (2026): High-Resolution Monitoring of Badland Erosion Dynamics: Spatiotemporal Changes and Topographic Controls via UAV Structure-from-Motion.– Water, 18/2, 234. https://doi.org/10.3390/w18020234

CROATIAN GEOLOGICAL SURVEY (2009): Geološka karta Republike Hrvatske M 1:300 000 [*Geological Map of the Republic of Croatia M 1:300 000* – in Croatian].– Croatian Geological Survey, Zagreb.

ĆOSOVIĆ, V., MARJANAC, T., DROBNE, K. & MORO, A. (2008): Outer Dinarides: eastern Adriatic coast. Paleogene and Neogene.– In: McCANN, T. (ed.): The Geology of Central Europe, Volume 2: Mesozoic and Cenozoic. The Geological Society London, London, 1031–1139.

GAMBLE, J.C. (1971): Durability-plasticity classification of shales and other argillaceous rocks.– Unpublished PhD Thesis, University of Illinois at Urbana-Champaign, 322 p.

GALLART, F., SOLÉ-BENET, A., PUIGDEFÁBREGAS, J. & LÁZARO, R. (2002). Badland systems in the Mediterranean.– In: BULL, J.L. & KIRKBY, M.J. (eds.): Dryland rivers: Hydrology and geomorphology of semi-arid cannels. John Wiley & sons, Ltd., 299–326.

GOKCEOGLU, C. & AKSOY, H. (2000): New approaches to the characterization of clay-bearing, densely jointed and weak rock masses.– Engineering Geology, 58/1, 1-23. https://doi.org/10.1016/S0013-7952(00)00032-6

GULAM, V. (2012): Erozija ogolina u flišu središnje istre [*The erosion of flysch badlands in the Central Istria* – in Croatian, with an English Abstract].– Unpublished PhD Thesis, Faculty of Mining, Geology and Petroleum Engineering, University of Zagreb, 275 p.

GULAM, V., GAJSKI, D. & POLLAK, D. (2018): Photogrammetric measurement methods of the gully rock wall retreat in Istrian Badlands.– Catena, 160, 289–309. https://doi.org/10.1016/j.catena.2017.09.024

GULAM, V., PETRINJAK, K., FRANGEN, T. & BOSTJANČIĆ, I. (2023): Field trip A1 – Grey Istria.– In: FIO FIRI, K. & ČOBIĆ, A. (eds.): Excursion guide – book. 7th Croatian geological congress with international participation, Zagreb, October 2–4. Croatian Geological Survey, 16–32.

GULAM, V., POLLAK, D. & PODOLSZKI, L. (2014): The analysis of the flysch badlands inventory in central Istria.– Croatia. Geologia Croatica, 67/1, 1–15. https://doi.org/10.4154/GC.2014.01

HARVEY, A. (2004). Badland.– In: GOUDIE, A.S. (ed.): Encyclopedia of geomorphology, Volume 1.– Routledge, Taylor & Francis Group, London and New York, 45–48.

HEAD, K.H. (1982): Manual of Soil Laboratory Testing, Vol 1: Soil Classification and Compaction tests, 3rd Edition.– CRC Press, Taylor & francis Group, London Plymouth, 422 p.

HORVAT, M., TOMAŠIĆ, N., ALJINOVIĆI, D., BUCKOVIĆI, D., ĆORIĆI, S., ĆOSOVIĆ, V., FELJA, I., GALOVIĆ, I., IŠTUK, Ž., KAMPIĆ, Š., KURTANJEK, D. & PEZELJ, Đ. (2023): Eocene Weathering Oscillations Imprinted in Marl Mineral and Geochemical Record (Dinaric Foreland Basin, Croatia).– Journal of Earth Science, 36, 1236-1250. https://doi.org/10.1007/s12583-023-1913-2

HOWARD, A.D. & KERBY, G. (1983): Channel changes in badlands.– Bulletin of the Geological Society of America, 94/6, 739–752. https://doi.org/10.1130/0016-7606(1983)94<739:CCIB>2.0.CO;2

HUDSON, N.W. (1993): Field measurement of soil erosion and runoff.– Food and Agriculture Organization of the United Nations, Rome, 139 p.

ISRM (1977): Suggested methods for determining water content, porosity, density, absorption, swelling and lake-durability index properties.– International Society for Rock Mechanics.

JURAČIĆ, M. (1979): Dubina sedimentacije "lapora s rakovicama" iz odnosa planktonskih i bentičkih foraminifera [*The depth of sedimentation of "marl with crabs" from the relation of planktonic and benthic foraminifera* – in Croatian].– Geološki vjesnik, 31, 61–67.

JUS (1982): Ispitivanje prirodnog kamena – Otpornost na dejstvo mraza [in Serbian].– Pravilnik br. 50-5823/1 od 1982-04-08, Službeni list SFRJ, br. 29/82. Savezni zavod za standardizaciju.

KASANIN-GRUBIN, M. & BRYAN, R. (2007): Lithological properties and weathering response on badland hillslopes.– Catena, 70, 68–78. https://doi.org/10.1016/j.catena.2006.08.001

KORBAR, T. (2009): Orogenic evolution of the External Dinarides in the NE Adriatic region: a model constrained by tectonostratigraphy of Upper Cretaceous to Paleogene carbonates.– Earth-Science Reviews, 96, 296–312. https://doi.org/10.1016/j.earscirev.2009.07.004

LETORTU, P., JAUD, M., GRANDJEAN, P., AMMANN, J., COSTA, S., MAQUAIRE, O., DAVIDSON, R., LE DANTEC, N. & DELACOURT, C. (2018): Examining high-resolution survey methods for monitoring cliff erosion at an operational scale.– GIScience and Remote Sensing, 55/4, 457–476. https://doi.org/10.1080/15481603.2017.1408931

MAGDALENIĆ, Z. (1972): Sedimentologija fliških naslaga Srednje Istre [*Sedimentology of Central Istria flysch deposits* – in Croatian, English Abstract].– Acta Geologica – VII/2, 39, 71–99.

MARINČIĆ, S., ŠPARICA, M., TUNIS, G. & UCHMAN, A. (1996): The eocene flysch deposits of the Istrian peninsula in Croatia and Slovenia. Regional, stratigraphic, sedimentological and ichnological analysis.– Annales Histoire Sciences Sociales, 9, 139–156.

MARINOS, V. (2010): New proposed GSI classification charts for weak or complex rock masses.– Bulletin of the Geological Society of Greece, 43/3, 1248–1258. https://doi.org/10.12681/bgsg.11301

MARINOS, P.V. (2014): Tunnel behaviour and support associated with the weak rock masses of flysch.– Journal of Rock Mechanics and Geotechnical Engineering, 6/3, 227–239. https://doi.org/10.1016/j.jrmge.2014.04.003

MARJANAC, T. & ĆOSOVIĆ, V. (2000): Tertiary depositional history of Eastern Adriatic realm.– Vijesti Hrvatskog geološkog društva, 37/2, 93–103.

MATIČEC, D., VLAHOVIĆ, I., VELIĆ, I. & TIŠLJAR, J. (1996): Eocene limestones overlying Lower Cretaceous deposits of western Istria (Croatia): Did some parts of present Istria form land during the Cretaceous?– Geologia Croatica, 49/1, 117–127. https://doi.org/10.4154/GC.1994.46

MCCOOL, D.K., DOSSETT, M.G. & YECHA, S.J. (1981): A portable rill meter for field measurement of soil loss.– In: Erosion and sediment transport measurement, Proceedings of the Florence Symposium, June 22–26. IAHS Publication, 133, 479–484.

MORENO-DE LAS HERAS, M. & GALLART, F. (2018): The origin of badlands.– In: NADAL-ROMERO, E. (ed.): Badlands dynamics in a context of global change. Elsevier Inc., 27–59. https://doi.org/10.1016/B978-0-12-813054-4.00002-2

MULDINI-MAMUŽIĆ, S. (1964): Mikrofauna vapnenaca i klastičnog razvoja paleogena Srednje Istre [*Microfauna of limestones and clastic development of the Paleogene of Central Istria* – in Croatian].– Geološki vjesnik, 18, 281–289.

NEUGIRG, F., STARK, M., KAISER, A., VLACILOVA, M., DELLA SETA, M., VERGARI, F., SCHMIDT, J., BECHT, M. & HAAS, F. (2016): Erosion processes in calanchi in the Upper Orcia Valley, Southern Tuscany, Italy based on multitemporal high-resolution terrestrial LiDAR and UAV surveys.– Geomorphology, 269, 8–22. https://doi.org/10.1016/j.geomorph.2016.06.027

OTONIČAR, B. (2007): Upper Cretaceous to Paleogene forbulge unconformity associated with foreland basin evolution (Kras, Matarsko podolje and Istria; SW Slovenia and NW Croatia).– Acta Carsologica, 36/1, 101–120. https://doi.org/10.3986/ac.v36i1.213

PETRINJAK, K., BUDIĆ, M., BERGANT, S. & KORBAR, T. (2021): Megabeds in Istrian Flysch as markers of synsedimentary tectonics within the Dinaric foredeep (Croatia).– Geologia Croatica, 74/2, 99–120. https://doi.org/10.4154/gc.2021.07

PETRINJAK, K., ĆORIĆ, S., PREMEC FUĆEK, V., ŠPANIČEK, J. & BERGANT, S. (2026): Integrated Planktonic Foraminiferal and Calcareous Nannofossil Biostratigraphy of the Eocene Istrian Flysch (Dinaric Foreland, Croatia).– Newsletters on Stratigraphy. https://doi.org/10.1127/nos/0926

PIKE, R.J., EVANS, I.S. & HENGL, T. (2008): Geomorphometry: A Brief Guide.– In: HENGL, T. & REUTER, H.I. (eds.): Geomorphometry: Concepts, Software, Applications, Developments in Soil Science, 33, Elsevier, 1–28.

RAMIREZ, D.M. (1988): Indigenous soil conservation strategies in Philippine uplands farms.– Working Paper No. 1.– Environment and Polixy Institute, East-West Center, Honolulu, 1, 47.

SCHMID, S.M., BERNOULLI, D., FÜGENSCHUH, B., MATENCO, L., SCHEFER, S., SCHUSTER, R., TISCHLER, M. & USTASZEWSKI, K. (2008): The Alpine-Carpathian-Dinaridic orogenic system: correlation and evolution of tectonic units.– Swiss Journal of Geosciences, 101, 139–183. https://doi.org/10.1007/s00015-008-1247-3

ŠIKIĆ, D. & PLENIČAR, M. (1975): Osnovna geološka karta SFRJ 1:100 000. Tumač za list Ilirska Bistrica L 33-89 [*Basic Geological Map of SFRY 1:100 000. Explanatory notes for the Ilirska Bistrica sheet L 33-89* – in Croatian].– Institut za geološka istraživanja, Zagreb, Geološki zavod, Ljubljana, Savezni geološki zavod, Beograd, 51 p.

TARLAO, A., TUNIS, G. & VENTURINI, S. (2005): Dropstones, pseudoplanktonic forms and deep-water decapod crustaceans within a Lutetian condensed succession of central Istria (Croatia): relation to palaeoenvironmental evolution and palaeogeography.– Palaeogeography, Palaeoclimatology, Palaeoecology, 218/3–4, 325–345. https://doi.org/10.1016/j.palaeo.2004.12.023

TAYLOR, R.K. (1988): Coal measures mudrocks: composition, classification and weathering processes.– Quarterly Journal of Engineering Geology, 21/1, 85–99. https://doi.org/10.1144/GSL.QJEG.1988.021.01.06

VELIĆ, I., TIŠLJAR, J., VLAHOVIĆ, I., MATIČEC, D. & BERGANT, S. (2003): Evolution of the Istrian part of the Adriatic Carbonate Platform from the Middle Jurassic to the Santonian and Formation of the Flysch Basin during the Eocene: Main Events and Regional Comparison.– In: VLAHOVIĆ, I. & TIŠLJAR, J. (eds.): Field Trip Guidebook – 22nd IAS Meeting of Sedimentology, Opatija, September 17–-19, Croatian Geological Survey, 57–63.

VLAHOVIĆ, I., TIŠLJAR, J., VELIĆ, I. & MATIČEC, D. (2005): Evolution of the Adriatic Carbonate Platform: Palaeogeography, main events and depositional dynamics.– Palaeogeography, Palaeoclimatology, Palaeoecology, 220/3–4, 333–360. https://doi.org/10.1016/j.palaeo.2005.01.011

WAINWRIGHT, J. & BRAZIER, R.E. (2011): Slope systems.– In: THOMAS, D.S.G. (ed.): Arid zone geomorphology: Process, Form and Change in Drylands, 3rd Edition, John Wiley & sons, Ltd., 209–233. https://doi.org/10.1002/9780470710777

WHEATON, J.M., BRASINGTON, J., DARBY, S.E. & SEAR, D.A. (2010): Accounting for Uncertainty in DEMs from Repeat Topographic Surveys: Improved Sediment Budgets.– Earth Surface Processes and Landforms, 35, 136–156. https://doi.org/10.1002/esp.1886

WILKINSON, M.W., JONES, R.R., & WOODS, C.E. (2016). A comparison of terrestrial laser scanning and structure-from-motion photogrammetry as methods for digital outcrop acquisition.– Geosphere, 12/6, 1865–1880. https://doi.org/10.1130/GES01342.1

WILLIAMS, R.D. (2012): DEMs of Difference.– Geomorphological Techniques, British Society for Geomorphology, 2, 3.2, 1–17.

WILSON, J.P. & GALLANT, J.C. (2000): Terrain Analysis: Principles and Applications.– John Wiley & Sons, Inc., New York, 479 p.

WOOD, J. (1996): The Geomorphological Characterisation of Digital Elevation Models.– Unpublished PhD Thesis, Department of Geography, University of Leicester, UK, 466 p.